

Transfer of ions in forward osmosis process using reverse osmosis rejects as draw solution and industrial wastewater as feed water

Ibrahim A. Alsayer^{a,*}, Ali A. Merdaw^b, Ibrahim S. Al-Mutaz^c

^aDepartment of Chemical Engineering, Northern Border University, Arar, Saudi Arabia, Tel. +9666634563; email: I.Alsayer@nbu.edu.sa

^bME Scientific Engineering Ltd., Leeds, West Yorkshire, United Kingdom, Tel. +441134406997; email: a.merdaw@mescieng.co.uk

^cChemical Engineering Department, College of Engineering, King Saud University, Saudi Arabia, Tel. +966114676870; email: almutaz@gmail.com

Received 17 November 2021; Accepted 9 June 2022

ABSTRACT

Forward osmosis (FO) is the engineered term of the natural process of osmosis, where water transfers naturally across a semi-permeable membrane from a low salinity solution, called feed water (FW), towards a high salinity solution, called draw solution (DS). An important potential application of FO is the dilution of the concentrated rejects of reverse osmosis (RO) processes by the low salinity industrial or municipal wastewaters. However, this transfer of freshwater from the FW to the DS is accompanied with another mutual transfer of multiple organic and inorganic ions. The ions transfer may affect the quality of the produced water and exceed the required limits of specifications. Currently, there is lack of information in the literature describing multiple ions transfer in actual FO processes utilizing real solutions. Most of the literature published so far discusses transport phenomena using specific binary system solutions. This study aims to provide an informative assessment of the transfer of ions between the FO membrane sides using the reject of an RO desalination process as DS, and a mixed wastewater obtained from an industrial mining site as FW. The experiments were conducted at a constant temperature of ~24°C and using a purpose made bench-scale osmotic cell. A symmetric cellulosic membrane, having a molecular weight cut-off of 3,500 Da, equivalent to a membrane mean pore diameter of about 2.8 nm, was utilized. The results show that the tested ions transferred at different rates across the membrane depending on their nature and concentration differences.

Keywords: Forward osmosis; Semi-permeable membranes; Water treatment; Desalination

1. Introduction

The provision of drinkable water supplies through desalination of sea and ground water and through treatment of industrial or municipal wastewater is one of the most significant challenges that the World faces. Solutions, including traditional water resources management techniques and water resources developments, will not suffice to

address future water problems. In the meantime, energy consumption becomes a major factor determining feasibility of the process, considering plant capital/operational costs and environmental impacts. Hence, membrane separation processes were attractive in this field of water industry due to their simplicity and low energy needs [1].

Forward osmosis (FO) is a membrane separation process where water is transferred naturally across a semi-permeable

* Corresponding author.

membrane from a low salinity solution, called feed water (FW), such as brackish water or wastewater, towards a high salinity solution, such as seawater or concentrated brine, called draw solution (DS). FO process is eco-friendly and consumes very little energy. The interest in FO technology over the past two decades has increased resulting in enormous publications in this field [2]. The main trends of research and development are investigations on new membranes, draw solutions, and optimizing the operational conditions. An ideal DS should provide high osmotic pressure, low viscosity, easy recovery, and non-toxicity [3].

Water is transferred in FO driven by a net differential pressure (NDP). The NDP is the sum of the hydrostatic pressure difference, ΔP , and the osmotic pressure difference, $\Delta \Pi$, between the membrane sides. Most FO applications are carried out at atmospheric or very low pressure; hence, the ΔP is usually neglected, and the NDP is considered as the $\Delta \Pi$ only. FO has many existing as well as potential applications. It is currently utilized in haemodialysis (dialysis) to purify blood from waste products, such as urea and excess water, and for several industrial purposes, such as concentrating of fruit juice and dairy products. This membrane processes is attractive to the industry due to its simplicity, where no phase change occurs, applications diversity at the ambient temperature, and the relatively low energy needs, which have a major impact on cost and greenhouse gases reduction [4–6].

One of the major problems facing the use of FO in industry is the need for efficient semi-permeable membranes with high water permeability, but having high solute rejection and good chemical stability. The membranes could be symmetric composed of one dense layer or asymmetric composed of several layers, usually a very thin skin, an intermediate layer, and a thicker substrate. Most of the membranes available in the market nowadays are designed for pressure-driven separation applications, and therefore, they are made asymmetric in order to withstand high hydrostatic pressure values. The symmetric membranes outperform the asymmetric ones for FO applications, as adding porous supports decreases water permeation excessively [7]. Symmetric membranes do not endure internal solute concentration polarization, which may occur in the substrate and the intermediate layer of the asymmetric membranes [8]. The synthesis of high performance FO membrane is still in the early stage of its development, and therefore, asymmetric membranes are currently used in FO studies and applications.

In the applications of wastewater treatments, utilizing FO process has many advantages. For example, the wastewater is concentrated by FO and reduced in volume. This will accordingly decreases the process feed flow-rate, reducing the plant size and its capital/operational costs. The extraction of freshwater from the wastewater can be achieved by utilizing a high salinity DS, such as seawater or the reject of a reverse osmosis (RO) or nanofiltration desalination process. The diluted DS can then be directly used for irrigation, for example, depending on its final specifications. Alternatively, diluted DS can be treated through other regeneration processes to recover the freshwater.

This study is a part of a project aims to develop a new technology integrating FO with an existing RO desalination

process to serve an industrial mining wastewater treatment (WWT) plant based in north Saudi Arabia. The RO process desalinates underground brackish water. The by-product of the RO process, the rejected concentrated brine, is a present ecological problem. The RO desalination plant produces, on average, 1.5 L of waste brine for every one liter of product freshwater output, that is, with 40% feed recovery rate. On the other hand, large quantities of freshwater are wasted and much energy is consumed by the WWT plant. This research project aims to turn the ecological problem of the RO rejected brine to an economic opportunity to recover the wasted freshwater during wastewater treatment.

Utilizing FO process in the above mentioned application involves reciprocal transfer of the dissolved ions between the DS and the FW. The solute transfer depends on its nature and the concentration difference across the membrane. It also depends on the membrane microstructure and the operational conditions. The transfer of ions may affect the specifications of the produced diluted DS or the recovered freshwater, as it is required to meet the end use specification. These specifications would determine the type of the regeneration process and their pre-treatment units.

Currently, there is lack of information in the literature describing multiple ions transfer in actual FO processes utilizing real solutions. Most of the literature published so far discusses transport phenomena in specific binary system solutions, such as sodium chloride-water solution. This study provides an informative assessment and attempts to provide better understanding of the multiple ions transfer between the FW and the DS as a function of the operational time. This study is a bench scale FO experimental work as a first step preparing for further developments of a pilot plant and commercializing. In this work, samples of the brine reject of the RO process is used as DS, while samples of the raw wastewater is used as FW. The FO membrane used in this study is a symmetric dialysis cellulosic membrane, available in the market, has a molecular weight cut-off (MWCO) value of 3,500 Da. The use of this type membrane was tested in two previous studies by the same group of researchers [9,10] and found to be suitable for FO applications.

1.1. Theory of FO

The phenomenon of osmosis (from the Greek word for 'push') is the transfer of a pure solvent towards its solution separated from it by a semi-permeable membrane. From a thermodynamic point of view, this operation is regarded as a non-equilibrium state. The hydrostatic pressure that must be applied to the solution to stop the influx of solvent is the value of its osmotic pressure, Π . Equilibrium is attained when the hydrostatic pressure of the solution equals the osmotic pressure, or when the osmotic pressures of the two solutions placed across the membrane are equal [11].

The currently available models for the mass transfer in FO are limited, but because the process shares many similarities with pressure-driven membrane processes, such as RO, models developed in this area have been used with different levels of validity [12]. However, these adapted models, similarly to that of the RO process, deal separately with the

transfer phenomena inside the membrane from that in the feed or the draw solutions.

Water is transferred by osmosis across a semi-permeable membrane from the FW to the DS driven by the NDP achieved by osmotic pressure difference, $\Delta\Pi$. Water transfers by pore flow through the membrane pores and by diffusion through the membrane dense material driven by osmosis, while the DS solute molecules are transferred in the opposite direction from the DS to the FW, driven by the concentration difference across the membrane [7,13].

1.1.1. Water flux

Water volumetric flux, J_w , can be defined by an extended version of Darcy's law [12,14] as follows:

$$J_w = \frac{\Delta P - \Delta\Pi_m}{\mu R_m} \quad (1)$$

where ΔP is the hydrostatic pressure difference, $\Delta\Pi_m$ is the osmotic pressure difference across the membrane material, μ is the fluid viscosity, and R_m is intrinsic resistance of the membrane material. By ignoring the ΔP , and replacing the term $(1/\mu R_m)$ by A_w , the membrane permeability coefficient, this equation can be written as follows:

$$J_w = A_w (\Pi_{DS} - \Pi_{FW}) \quad (2)$$

That is by assuming that the osmotic pressure difference across the membrane material is the same as that between the two solutions, $\Pi_{DS} - \Pi_{FW}$. Water flux can be expressed in units of, for example, $L/m^2 h$, where A_w is a water permeability coefficient with units of, for example, $L/m^2 h \text{ bar}$.

The osmotic pressure of the solution is usually estimated using van't Hoff equation for ideal solutions [15]:

$$\Pi = i_v \frac{C}{M_{wt}} R_g T \quad (3)$$

where i_v is the van't Hoff factor and refers to the number of moles of the dissociated entities when one mole of the solid solute is dissolved (e.g., 2 for NaCl), c is the weight concentration of the solute, M_{wt} is the molecular weight, R_g is the universal gas constant, and T is the thermodynamic temperature.

In ionic solutions, due to a phenomenon called ion pairing, a certain number of the positive and the negative ions will randomly come together and form ion pairs. This reduces the total number of free particles in solution, and consequently decreases the osmotic pressure from its ideally estimated value by Eq. (3). This effect can be considered by introducing the osmotic coefficient, \emptyset , which accounts for the deviation of the solvent from the ideal behaviour. The osmotic coefficient is defined as [16]:

$$\emptyset = \frac{\mu_A^* - \mu_A}{R_g T \ln(x_A)} \quad (4)$$

where μ_A^* and μ_A are the chemical potentials of the solvent as a pure substance and in solution, respectively, and

x_A is the solvent mole fraction. The osmotic coefficient is sometimes called the rational osmotic coefficient.

Hence, Eq. (3) can be rewritten by incorporating \emptyset to give:

$$\Pi = \emptyset i_v \frac{C}{M_{wt}} R_g T \quad (5)$$

The value of \emptyset usually falls within the range of $0 < \emptyset < 1$, where 1 indicates 100% ions dissociation. However, \emptyset can also be larger than 1 (e.g., for sucrose and glycerol). For ionic salts, the electrostatic effects cause \emptyset to be smaller than 1 even if 100% dissociation occurs.

1.1.2. Solute flux

The DS solute mass flux, J_s , can be represented as:

$$J_s = B_s (c_{DS} - c_{FW}) \quad (6)$$

The DS solute mass flux, with units of, for example, $g/m^2 h$, is driven by the concentration difference $(c_{DS} - c_{FW})$, in, for example, g/m^3 , where B_s is a DS solute permeability coefficient with units of, for example, m/h .

The solute permeability, B_s , can be described by a well-known model for the mass transfer through dense membranes, the solution-diffusion (SD) model [17]. This model applies to RO, pervaporation, gas permeation and dialysis processes in polymeric membranes. Despite the apparent difference between these processes, all of them involve diffusion of molecules in a dense polymer, but under different driving forces. Any of the driving forces, the pressure, the temperature, and the concentration on both sides of the semi-permeable membrane determines the concentration gradient of the diffusing species.

The SD model is solidly built on thermodynamics, that the driving force of pressure, temperature, concentration, and the electrical potential are interconnected. The overall driving force generates a gradient of chemical potential, which determines the permeation across the membrane. Thus the flux of the solute, J_s , can be described by the following relationship:

$$J_s = -L_s \frac{d\mu_s}{dx} \quad (7)$$

where $d\mu_s/dx$ is the chemical potential gradient of the solute and L_s is a proportionality coefficient, which is not necessarily constant. The chemical potential for concentration and pressure gradient as driving force can be written as:

$$d\mu_s = R_g T d \ln(\gamma_s n_s) + v_s dP \quad (8)$$

where n_s is the mole fraction of the solute (mole/mole), γ_s is the activity coefficient (mole/mole) linking mole fraction to activity, P is the pressure, and v_s is molar volume of the solute.

For incompressible liquids having constant volume, Eq. (8) can be integrated with respect to concentration and pressure as follows:

$$\mu_s = \mu_s^o + R_g T \ln(\gamma_s n_s) + v_s (P - P_s^o) \quad (9)$$

where μ_s^o is the chemical potential of the pure solute at a reference pressure, P_s^o , which can be defined in this case as the saturation vapour-pressure of the solute.

By assuming constant activity coefficient for the solute, γ_s , Eq. (8) can be substituted in Eq. (7) to produce the following:

$$J_s = -\frac{R_g T L_s}{n_s} \frac{dn_s}{dx} \quad (10)$$

According to the SD model, Eq. (10) has been modelled for permeation by assuming: (a) the fluids on either side of the membrane are in equilibrium with the interface of the membrane material and the rate of diffusion through the membrane is much lower than the rates of absorption and desorption at the interface, and (b) the pressure across the membrane, if applied, is constant and takes the highest value of either side; this assumes that the pressure is uniform within the membrane and the chemical potential gradient across the membrane is expressed only by the concentration gradient.

In Eq. (10), the gradient of solute species is represented by n_s , which is the mole fraction. In order to use better practical form, the weight concentration of the solute, c , can be introduced:

$$c = M_{wt} \rho n_s \quad (11)$$

where c has units of, for example, g/L, M_{wt} is the molecular weight of the solute, in, for example, g/mol, and ρ is the molar density of the solution with units of, for example, mol/L.

Hence, Eq. (10) can be written as:

$$J_s = -\frac{R_g T L_s}{c} \frac{dc}{dx} \quad (12)$$

The term $(R_g T L_s / c)$ in Eq. (12) is analogous to the diffusivity of the solute inside the membrane, D_{sm} , in Fick's law, thus:

$$J_s = -D_{sm} \frac{dc}{dx} \quad (13)$$

For comparison, the values of the diffusion coefficients of some inorganic cations, inorganic anions, and organic ions at infinite dilution, D_f , are listed in Table 1, noting that the diffusivity inside the membrane material is lower than that in the diluted solution, and that the diffusivity decreases as the solute concentration increases. However, it can be indicated from Eq. (13) that solute flux is proportional to the solute diffusivity, while it decreases by increasing the membrane thickness. This can also explain the effect of fouling at the membrane surface, as it increases the actual membrane thickness. The transfer of solutes, as well as water flux, decreases as the membrane fouling increases.

By integrating Eq. (13) over the thickness of the membrane, δ_m , the following relationship can be obtained:

$$J_s = -\frac{D_{sm}}{\delta_m} (c_{0-m} - c_{\delta-m}) \quad (14)$$

where c_{0-m} and $c_{\delta-m}$ are the solute concentrations at the membrane interfaces at both sides (FW and DS, respectively).

The above modelling is analogous to the FO process across the membrane dense material only. However, the concentration at the bulk fluid can be related to that at the membrane interface by equating their chemical potentials, that is, by using Eq. (9), which produces the following at both sides of the membrane:

$$\ln(\gamma_s n_s) = \ln(\gamma_{s-m} n_{s-m}) \quad (15)$$

and thus:

$$n_{s-m} = \frac{\gamma_s}{\gamma_{s-m}} n_s \quad (16)$$

By substituting in Eq. (11):

$$c_m = \frac{\gamma_s \rho_m}{\gamma_{s-m} \rho} c \quad (17)$$

Eq. (17) can be simplified by defining a solute sorption coefficient, K_{sm} , assumed equal at both sides of the membrane, hence:

$$c_m = K_{sm} c \quad (18)$$

Now by substituting Eq. (18) in Eq. (14), the relationship for solute flux can be written as follows:

$$J_s = -\frac{D_{sm} K_{sm}}{\delta_m} (c_0 - c_\delta) \quad (19)$$

The product $(D_{sm} K_{sm})$ is referred to as the solute permeability coefficient, B_s , in some references [17]; however, it is more common to use the whole term $(D_{sm} K_{sm} / \delta_m)$ as the B_s and thus Eq. (19) can be rewritten as:

$$J_s = B_s (c_\delta - c_0) \quad (20)$$

Eq. (20) is the same as Eq. (6) and implies the use of the average values of the diffusivity and the sorption coefficient over the membrane thickness [17].

The model described above accounts for the mass transfer through the membrane dense material in symmetric membranes, or the skin active layer in asymmetric membranes; it is unable to describe or to predict all of the phenomena associated with this process [20]. However, the concentration polarization (CP) model is suggested in literature to describe mass transfer in the membrane porous substrate or the fluid film alongside the membrane surface. CP model simplifies the problem by assuming several ideal behaviours for the fluid. Estimation of CP

Table 1
Diffusion coefficients, D_i , of some ionic solutes at infinite dilution

Inorganic cations			
Cation	Charge of ion	$D_i/10^{-9}$ (m ² /s)	References
Ag	+1	1.648	[18]
Al	+3	0.559	[19]
Ba	+2	0.848	[19]
Be	+2	0.599	[18]
Ca	+2	0.793	[19]
CaHCO ₃	+1	0.506	[19]
Cd	+2	0.717	[19]
Co	+2	0.732	[18]
Cr	+3	0.595	[18]
Cu	+2	0.733	[19]
Fe	+2	0.719	[19]
Fe	+3	0.604	[18]
H	+1	9.310	[19]
Hg	+2	0.913	[18]
K	+1	1.960	[19]
Li	+1	1.030	[19]
Mg	+2	0.705	[19]
MgHCO ₃	+1	0.478	[19]
Mn	+2	0.688	[19]
Na	+1	1.330	[19]
NH ₄	+1	1.980	[19]
Pb	+2	0.945	[19]
Sr	+2	0.794	[19]
UO ₂	+2	0.426	[18]
Zn	+2	0.715	[19]
Inorganic anions			
Anion	Charge of ion	$D_i/10^{-9}$ (m ² /s)	References
Br	-1	2.010	[19]
Cl	-1	2.030	[19]
CO ₃	-2	0.955	[19]
CN	-1	2.077	[18]
CNO	-1	1.720	[18]
CrO ₄	-2	1.132	[18]
F	-1	1.460	[19]
H ₂ AsO ₄	-1	0.905	[18]
H ₂ PO ₄	-1	0.846	[19]
HCO ₃	-1	1.180	[19]
HPO ₄	-2	0.690	[19]
HS	-1	1.730	[19]
HSO ₄	-1	1.330	[19]
I	-1	2.045	[19]
KSO ₄	-1	0.746	[19]
MnO ₄	-1	1.632	[18]
MoO ₄	-2	1.984	[18]
NaCO ₃	-1	0.585	[19]
NaSO ₄	-1	0.618	[19]
NO ₂	-1	1.910	[19]

Inorganic anions			
Anion	Charge of ion	$D_i/10^{-9}$ (m ² /s)	References
NO ₃	-1	1.900	[19]
OH	-1	5.270	[19]
PO ₄	-3	0.612	[19]
S	-2	0.731	[19]
SeO ₄	-2	1.008	[18]
SO ₄	-2	1.070	[19]
Organic anions			
Organic anion	Charge of ion	$D_i/10^{-9}$ (m ² /s)	References
Acetate	-1	1.089	[18]
Benzoate	-1	0.863	[18]
Butyrate	-1	0.868	[18]
Citrate	-3	0.623	[18]
Dihydrogen citrate	-1	0.799	[18]
Formate	-1	1.454	[18]
Hydrogen oxalate	-1	1.070	[18]
Isovalerate	-1	0.871	[18]
Lactate	-1	1.033	[18]
Malate	-2	0.783	[18]
Maleate	-2	0.824	[18]
Oxalate	-2	0.987	[18]
Phenyl acetate	-1	0.815	[18]
o-Phthalate	-2	0.696	[18]
m-Phthalate	-2	0.728	[18]
Pivalate	-1	0.849	[18]
Salicylate	-1	0.959	[18]
Suberate	-2	0.479	[18]
Succinate	-2	0.783	[18]
Tartarate	-2	0.794	[18]

effect requires applying numerically a suitable empirical relationship (Sherwood correlation) to calculate the mass transfer coefficient through the fluid thin film. The mass transfer correlations are usually borrowed from non-porous smooth duct flow, and therefore their application in the case of membrane operation has been criticized, since neither membrane's porosity nor diffusivity due to CP are taken into consideration [21]. However, a combination is used in the literature to join the CP model with the membrane models, for example, the SD model [12]. This combination was found to represent the experimental results rather poorly. Therefore, there is still a need to develop new analytical mass transfer models that combine both the fluid properties and the membrane micro-structural parameters, and account for diffusion and pore flow characteristics.

All concentration polarization phenomena have negative effect on the obtainable water flux through membranes

due to the drop in the net osmotic pressure driving force. In osmotic processes, mass transfer is critical on both sides of the membrane. As indicated earlier, most of the membranes currently used in FO processes are asymmetric composed of several layers (active layer, intermediate layer, and porous substrate layer). The porous substrate of the membrane exerts a negative effect on the water flux, as an internal concentration polarization (ICP) may take place. The ICP occurs in one of two manners, dilutive (DICP) or concentrative (CICP), within the porous substrate depending on which side of the substrate is against the DS or the FW. Hence, using dense membranes composed of one single active layer would improve the FO processes performance.

2. Materials and methods

2.1. FO membrane

The FO membrane used in this study is a dialysis cellulose membrane, supplied by Medicell International Ltd., (UK), type DVT03500. This membrane has a molecular weight cut-off (MWCO) value of 3,500 Da. According to the manufacturer datasheets, this membrane is made of natural cellulose (cotton linters). It is fabricated by dissolving cellulose in special inorganic solvents, the polymer then reformed by taking away the solvent to form the membrane as a flat sheets or tubes. This membrane is highly resistant to organic solvents, elevated temperatures, and extremes of pH. It is made of one dense layer with an average thickness of 77 μm .

The name code of the membrane DVT03500 refers to its MWCO, which is 3,500 Daltons. It has a mean pore diameter of about 2.8 nm, as calculated using the following empirical relationship between the molecular weight and the molecular diameter [22]:

$$D_p = 0.066M_{wt}^{0.46} \quad (21)$$

where D_p is the approximate diameter of the molecule in nano-meters and M_{wt} is the molecular weight in g/mol.

Most of the FO studies published so far utilize RO asymmetric membranes with thinner active layers and smaller mean pore diameters, for example, 0.25–0.30 nm [23]. This study investigates the FO process using a dialysis membrane with larger mean pore diameter and made of one single dense layer in order to avoid the effects of the ICP.

2.2. Osmotic cell

The FO process is investigated in this study using the set-up schematically represented in Fig. 1. It is composed of two plastic (PVC) tanks; the first tank is an osmotic cell has a capacity of 18 L contains the DS, while the other tank has a capacity of 15 L contains the FW. Each tank is equipped with a tap and a water level indicator. The FO cell is composed of 12 parallel membrane tubes arranged horizontally in three rows by four columns. The length of each membrane tube is 300 mm with a diameter of 16 mm. The membrane tubes are connected between the DS tank sides submerged under the level of the DS solution. It is designed that the FW flows inside the membrane tubes,

while the DS on the outside. The total surface area of the membrane is calculated to be 0.181 m². The inlets and outputs of the membrane tubes are collected outside the DS tank using a configuration of connectors and plastic tubes.

Each of the DS and the FW tanks are equipped with a small submersible pump; the first pump circulates the DS solution inside the DS tank homogenising the solute concentration, while the other pump circulates the FW between the two tanks through the tubular membranes. The flow rate of the DS pump is 10 L/min, while the flow rate of the FW pump is 7.44 L/min; both pumps are of about 1 m head. The average FW flow rate inside each tubular membrane is 0.62 L/min, providing a laminar flow pattern with a Reynolds number value of about 922.

2.3. Specifications of the FW and the DS

Industrial mixed wastewater, comparable to brackish water, obtained from a mining site was used as FW, while a concentrated RO reject of a groundwater desalination process was used as DS. Several FO runs, 10 runs in total, were conducted using the same starting solutions. All experiments and tests were carried out at similar operational conditions and ambient temperature (~24°C). Some of the FO runs lasted for 5 h, while others stopped after 1, 2, 3, or 4 h, in order to take enough samples for the chemical analyses of the diluted DS. The average mean of the experimental results was considered to record the readings taken at the similar times.

2.4. Measuring methods

Water flux was calculated experimentally by dividing the DS volume increase ($V_2 - V_1$) by the membrane area (A_m) and the relevant time difference ($t_2 - t_1$), as follows:

$$J_w = \frac{V_2 - V_1}{A_m(t_2 - t_1)} \quad (22)$$

The concentration measurements of the ions in the FW and the DS, as well as the other solution properties (pH, temperature, electrical conductivity, total dissolved solids, and turbidity), were obtained using the following laboratory equipment: (1) pH and temperature: HQ11D Digital pH meter by Hach (USA), providing 0.01 pH and $\pm 0.3^\circ\text{C}$ temperature accuracy, (2) electrical conductivity and total dissolved solids (TDS): ULTRAMETER II 6PFC^E by Myron L Company (USA), providing an accuracy of $\pm 1\%$ of electrical conductivity and TDS readings, (3) concentrations of ions: DR6000 UV-VIS Spectrophotometer by Hach (USA), and (4) turbidity: 2100Q-IS Turbidimeter by Hach, providing an accuracy of $\pm 1\%$ of readings. The total alkalinity of the solutions was measured using the titration method with sulphuric acid.

3. Results and discussions

Fig. 2 shows the average volumes of water transferred from the FW to the DS at the end of each hour of operation time. The average membrane water flux is calculated using

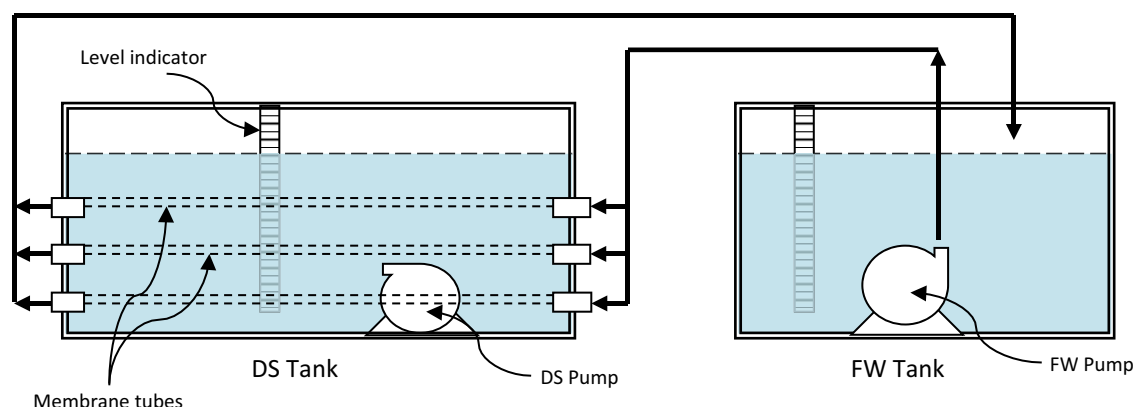


Fig. 1. Schematic representation for the FO bench-scale experimental setup.

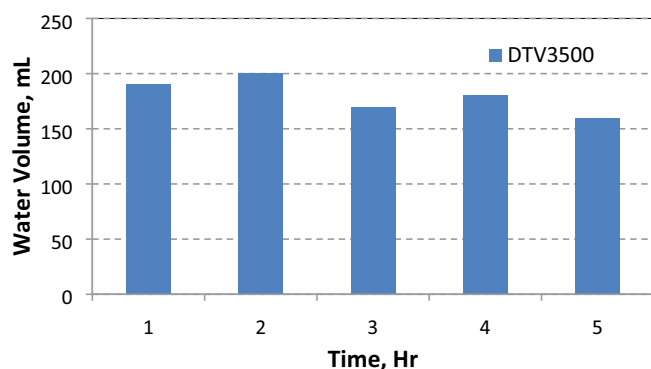


Fig. 2. Average volume of water transferred from the FW to the DS as a function of operational time utilizing the membrane DTV03500 in several FO experiments at $\sim 24^{\circ}\text{C}$.

Eq. (22) and found to be $1.09 \text{ L/m}^2 \text{ h}$. The trend of water volume increase, and water flux, was almost stable during the 5 h operation time; although, the small reduction in the osmotic pressure difference across the membrane, $\Delta\Pi$. On average, the $\Delta\Pi$ is decreased from 2.8 bar initially to 1.8 bar at the end of the 5 h run, as can be indicated from the data of Table 2. The approximate osmotic pressure values were calculated from the TDS readings using the van't Hoff Eq. (3) on the assumption of that the solution is ideal and the TDS is spread over Sodium (Na^+) and chloride (Cl^-) ions.

The freshwater recovered at the end of each of these FO runs was about 0.9 L. Accordingly, starting from an initial FW volume of 15 L, the recovery rate is calculated to be 6%. Similarly, from an initial DS volume of 18 L, the dilution rate of the DS is calculated to be 5%. These rates can be improved in practice by increasing the membrane area or the FW solution residence time, as can be explained in Eq. (22), or by increasing the membrane permeability and the osmotic pressure difference, as it is explained in Eq. (2).

Table 2 shows the specifications of the FW, the wastewater, at the initial conditions and after the end of the 5 h of operation. It also shows the conditions of the DS solution, the RO reject, initially and at the end of each of the 5 h of operation. The results show a consistent transfer of the ions across the FO membrane from high concentration

side to low concentration side. The tested ions were present at different concentrations in the FW and the DS at the start of the experiments. Free chlorine and total coliforms, by membrane filtration method, were also tested in the FW and the DS, but were not detected and, therefore, not shown in this table.

The total permanent hardness of water, expressed as equivalent of calcium carbonate, was calculated from the concentrations of the calcium ion, $[\text{Ca}^{2+}]$, and the magnesium ion, $[\text{Mg}^{2+}]$, using the following relationship, where M refers to the molecular weight:

$$[\text{CaCO}_3] = \frac{M_{\text{CaCO}_3}}{M_{\text{Ca}}} [\text{Ca}^{2+}] + \frac{M_{\text{CaCO}_3}}{M_{\text{Mg}}} [\text{Mg}^{2+}] \quad (23)$$

The properties and results listed in Table 2 are plotted in the following figures for more clarification. Fig. 3 shows the decreasing trend of the TDS at the DS side with time. The reduction is due to an obvious dilution effect of freshwater transfer from the FW to the DS. TDS at the DS decreased from 5,335 to 4,543 ppm, while it increased at the FW from 1,716 to 2,221 ppm. Ideally, the TDS increase at the DS should be equal to the decrease at the FW; however, due to that the TDS is more relevant to the electrical conductivity of the solution rather than the nature and the concentration of the dissolved species in the solution, considering the variety of the solutes present in these experiments, the TDS values should be considered as an indication only.

The results of ions concentrations show a normal trend of transfer across the membrane from a high concentration side to a low concentration side. As it is shown in Figs. 4–6, all the tested ions (chloride, sulphate, calcium, magnesium, nitrite, phosphate, iron, nitrate, and fluoride) diffused from the DS towards the FW opposite to the direction of water flux, except the ammonium ion, as shown in Fig. 5, diffused from the FW to the DS. The ammonium ion initial concentration at the FW side was higher than that at the DS, due to the nature of the wastewater used in this study, which is a mixture of industrial and municipal wastewaters discharged from an industrial mining site. The rate of the transfer of each ion depends on many

Table 2
Summary of the test results of properties and ion concentrations in both FW and DS solutions

#	Parameter	FW		DS					
		Initial	End	Initial	1 h	2 h	3 h	4 h	5 h
1	pH	8.36	8.4	8.13	8.08	8.07	8.06	8.05	8.04
2	Temperature, °C	24	23.7	24	24.1	24.3	24.5	24.5	24.5
3	Electrical conductivity, mS/cm	2.305	2.947	6.588	6.306	6.130	5.958	5.814	5.675
4	TDS, ppm	1,716	2,221	5,335	5,091	4,942	4,792	4,667	4,543
5	Osmotic pressure, bar	1.35	1.74	4.19	4.00	3.88	3.71	3.66	3.57
6	Turbidity, NTU	1.84	0.85	0.78	0.71	0.78	0.58	0.63	0.65
7	Total permanent hardness, ppm of CaCO ₃	1,261	1,831	3,839	3,772	3,580	3,535	3,362	3,280
8	Calcium, Ca ²⁺ , ppm	168	329	550	533	507	471	441	410
9	Magnesium, Mg ²⁺ , ppm	205	246	601	595	564	575	551	550
10	Total alkalinity, ppm	170	290	823	783	745	728	704	700
11	Chloride, Cl ⁻ , ppm	250	490	921	758	731	728	709	702
12	Nitrite, NO ₂ ⁻ , ppm	0.00	0.05	0.10	0.09	0.08	0.06	0.05	0.05
13	Ammonium, NH ₄ ⁺ , ppm	0.43	0.26	0.10	0.13	0.17	0.20	0.22	0.25
14	Phosphate, PO ₄ ³⁻ , ppm	0.05	0.33	0.61	0.56	0.45	0.40	0.38	0.35
15	Sulphate, SO ₄ ²⁻ , ppm	220	356	1,164	1,143	1,130	1,070	1,028	1,015
16	Iron, Fe ²⁺ , ppm	0.01	0.04	0.09	0.08	0.07	0.06	0.05	0.04
17	Nitrate, NO ₃ ⁻ , ppm	0.90	1.50	3.37	3.30	3.20	3.10	3.00	2.80
18	Fluoride, F ⁻ , ppm	0.65	1.60	3.31	2.55	2.5	2.48	2.44	2.44
19	Silica, SiO ₂ , ppm	12.0	18.0	26.0	25.0	23.0	22.0	22.0	21.0

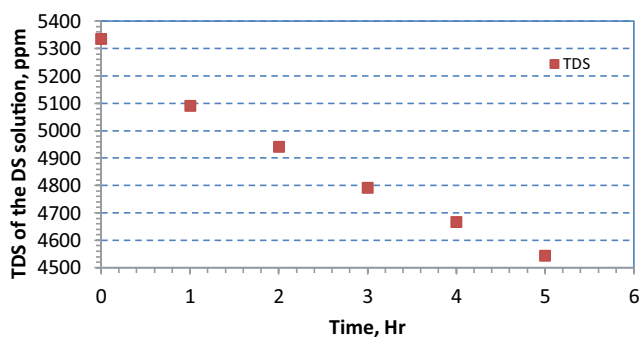


Fig. 3. TDS average values of the DS as a function of experiment time in several FO experiments carried out at ~24°C.

factors, such the ion specific diffusivity and the driving force of the concentration difference across the membrane.

The rate of the ion transfer depends also on the hydration properties of the ions; specifically, the activity or the hydration strength. In ionic solutions, the higher the charge density, the more heavily hydrated the ion, while the neutral molecules, for example, organic molecules, have weak linkages with water molecules. A suitable measure for the comparison between molecules in their extent of hydration is the value of the hydration number. For example, an experiment based on the ion transport through cellophane membrane gave the following hydration numbers for several inorganic ions, Li⁺: 22, Na⁺: 13, K⁺: 7, Cs⁺: 6, F⁻: 7, Cl⁻: 5, Br⁻: 5, SO₄²⁻: 12, Sr²⁺: 29, and Mg²⁺: 36. These particular results for the hydration numbers show the following trends: (a) cations have a tendency to be more hydrated

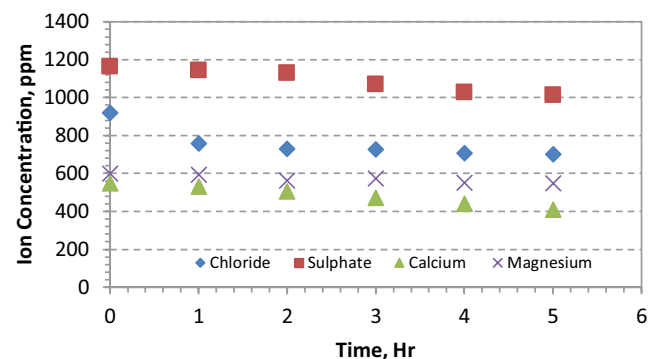


Fig. 4. Chloride, sulphate, calcium, and magnesium ions concentration in the DS as a function of experiment time in several FO experiments carried out at ~24°C.

than anions, (b) the greater the charge, the more heavily hydrated is the ion, and (c) for a given charge type, the smaller the crystal radii, the more heavy is the ion hydration [24].

4. Conclusions

In forward osmosis (FO) process water transfers naturally across a semi-permeable membrane from a low osmotic pressure side, the feed water (FW), to a high osmotic pressure side, the draw solution (DS). An important potential application of FO is the dilution of the concentrated rejects of reverse osmosis (RO) processes by freshwater extracted from industrial or municipal wastewaters.

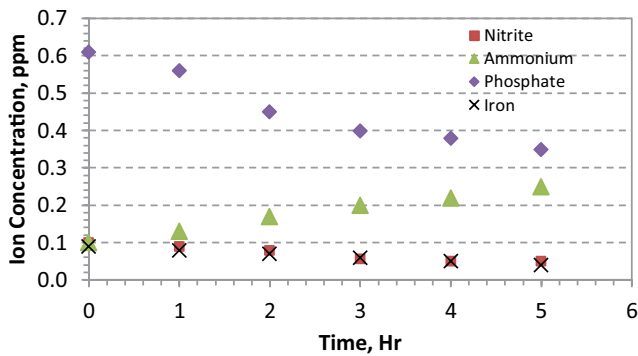


Fig. 5. Nitrite, ammonium, phosphate, and iron ions concentration in the DS as a function of experiment time in several FO experiments carried out at $\sim 24^{\circ}\text{C}$.

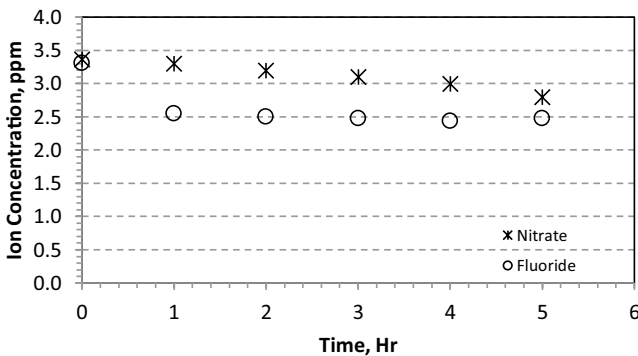


Fig. 6. Nitrate and fluoride ions concentration in the DS as a function of experiment time in several FO experiments carried out at $\sim 24^{\circ}\text{C}$.

The RO rejects has higher osmotic pressure than that of the wastewater; hence, water can be transferred using FO from the wastewater to the RO rejects. However, this transfer of freshwater is accompanied by another mutual transfer of the existing ions. Some ion concentrations may exceed the limits of the end use specifications and affect the quality of the produced water. This study investigates the transfer of ions between both sides of an FO membrane using real solutions. The experiments were conducted at a constant temperature of $\sim 24^{\circ}\text{C}$ and using a symmetric cellulose membrane has a molecular weight cut-off (MWCO) of 3,500 Daltons, equivalent to a membrane mean pore diameter of about 2.8 nm.

This study aims to provide an informative assessment. The results of this study in terms of water flux and ion transfer will be used as a guideline to design a pilot plant to implement this application. The by-product of the RO processes, the rejected concentrated brine, is a present ecological problem, while large quantities of freshwater are wasted and much energy is consumed by the WWT plants. This research project aims to turn the ecological problem of the RO rejected brine to an economic opportunity to recover the wasted freshwater during wastewater treatment.

The FO experiments were carried out using the reject of a ground-water RO desalination process as DS, while a

mixed wastewater discharged from an industrial mining site was used as FW. This study investigated the mutual transfer of ions between both sides of the FO membrane. The ions tested were calcium (Ca^{2+}), magnesium (Mg^{2+}), chloride (Cl^{-}), nitrite (NO_2^{-}), ammonium (NH_4^{+}), phosphate (PO_4^{3-}), sulphate (SO_4^{2-}), iron (Fe^{2+}), nitrate (NO_3^{-}), and fluoride (F^{-}). Other tests were also carried out for the pH, the electrical conductivity, the TDS, the turbidity, and the total alkalinity. The osmotic pressure of the solutions and the total permanent hardness were calculated using empirical equations. The count of coliforms and free chlorine were also tested, but not detected in both solutions.

The recovery achieved of freshwater from the FW at the end of each of these FO runs was about 0.9 L, starting from an initial FW volume of 15 L, that is, 6% recovery rate, while the achieved DS dilution rate, which is started at a volume of 18 L, was 5%. These rates can be improved in practice by increasing the membrane area, as well as by increasing the membrane permeability and/or the osmotic pressure difference. The recovery rates can also be increased by increasing the operational residence time; however, this may affect the quality of the produced solution due to continuous solute transfer.

The results of the ions' concentrations show a normal trend of transfer from the high concentration side to the low concentration side across the semi-permeable membrane. All the inspected ions (chloride, sulphate, nitrite, phosphate, iron, nitrate, and fluoride) diffused from the DS towards the FW opposite to the direction of water flux, except the ammonium ion diffused from the FW to the DS. The ammonium ion initial concentration at the FW side was higher due to the nature of the wastewater examined, which was a mixture of industrial and municipal wastewater discharged from a mining site.

Acknowledgement

The authors extend their appreciation to the Deputyship for Research & Innovation, Ministry of Education in Saudi Arabia for funding this research work through the project number 4426-2020-IF.

References

- [1] M.W. Shahzad, M. Burhan, L. Ang, K.C. Ng, Energy-water-environment nexus underpinning future desalination sustainability, *Desalination*, 413 (2017) 52–64.
- [2] J. Wang, X. Liu, Forward osmosis technology for water treatment: recent advances and future perspectives, *J. Cleaner Prod.*, 280 (2021) 124354, doi: 10.1016/j.jclepro.2020.124354.
- [3] Q. Ge, M. Ling, T.-S. Chung, Draw solutions for forward osmosis processes: developments, challenges, and prospects for the future, *J. Membr. Sci.*, 442 (2013) 225–237.
- [4] Z.L. Cheng, X. Li, T.-S. Chung, The forward osmosis-pressure retarded osmosis (FO-PRO) hybrid system: a new process to mitigate membrane fouling for sustainable osmotic power generation, *J. Membr. Sci.*, 559 (2018) 63–74.
- [5] K. Lutchimiah, A.R.D. Verliefde, K. Roest, L.C. Rietveld, E.R. Cornelissen, Forward osmosis for application in wastewater treatment: a review, *Water Res.*, 58 (2014) 179–197.
- [6] Z. Li, R. Valladares Linares, S. Sarp, G. Amy, Chapter 9 – Direct and Indirect Seawater Desalination by Forward Osmosis, S. Sarp, N. Hilal, Eds., *Membrane-Based Salinity Gradient Processes for Water Treatment and Power Generation*, 1st ed., Oxford, Elsevier, UK, 2018.

- [7] S. Loeb, L. Titelman, E. Korngold, J. Freiman, Effect of porous support fabric on osmosis through a Loeb-Sourirajan type asymmetric membrane, *J. Membr. Sci.*, 129 (1997) 243–249.
- [8] J.R. McCutcheon, M. Elimelech, Modeling water flux in forward osmosis: implications for improved membrane design, *AIChE J.*, 53 (2007) 1736–1744.
- [9] I.A. Alenezi, A.A. Merdaw, Proportionality of solute flux and permeability to water flux and permeability in forward osmosis process, *Desal. Water Treat.*, 225 (2021) 29–36.
- [10] I.A. Alsayer, A.A. Merdaw, I.S. Al-Mutaz, Effect of membrane mean pore diameter on water and solute flux in forward osmosis processes, *Int. J. Adv. Appl. Sci.*, (in Press).
- [11] J.T. Tinge, G.J.P. Krooshof, T.M. Smeets, F.H.P. Vergossen, J. Krijgsman, E. Hoving, R.M. Altink, Direct osmosis membrane process to de-water aqueous caprolactam with concentrated aqueous ammonium sulphate, *Chem. Eng. Process.*, 46 (2007) 505–512.
- [12] D. Hughes, T. Taha, Z. Cui, *Mass Transfer: Membrane Processes*, S.S. Sablani, A.K. Datta, M. Shafiur Rahman, A.S. Mujumdar, Eds., *Handbook of Food and Bioprocess Modeling Techniques*, CRC Press, Boca Raton (USA), 2006.
- [13] M.M. Pendergast, S.M. Nowosielski-Slepowron, J. Tracy, Going big with forward osmosis, *Desal. Water Treat.*, 57 (2016) 26529–26538.
- [14] S.E. Ingebritsen, W.E. Sanford, C.E. Neuzil, *Groundwater in Geologic Processes*, 2nd ed., University Press, Cambridge, 2006.
- [15] J.H. van't Hoff, The role of osmotic pressure in the analogy between solutions and gases, *Zeitschrift fur physikalische Chemie*, 1 (1887) 481–508.
- [16] A.D. McNaught, A. Wilkinson, *IUPAC Compendium of Chemical Terminology*, 2nd ed., The Gold Book, Blackwell Science, Oxford, UK, 1997.
- [17] R.W. Baker, *Membrane Technology and Application*, 2nd ed., John Wiley & Sons, Ltd., Chichester, UK, 2004.
- [18] P. Vanýsek, *Ionic Conductivity and Diffusion at Infinite Dilution*, *Handbook of Chemistry and Physics*, 1992/93 ed., CRC Press, Boca Raton, 1992, pp. (5–111)–(5–113).
- [19] PhreeqC (Version 3) – A Computer Program for Speciation, Batch-Reaction, One-Dimensional Transport, and Inverse Geochemical Calculations; [The Diffusion Coefficients are Taken from the Thermodynamic Database “phreeqc.dat”].
- [20] H. Mehdizadeh, J.M. Dickson, Modeling of reverse osmosis in the presence of strong solutemembrane affinity, *AIChE J.*, 39 (1993) 434–445.
- [21] S.S. Sablani, M.F.A. Goosen, R. Al-Belushi, M. Wilf, Concentration polarization in ultrafiltration and reverse osmosis: a critical review, *Desalination*, 141 (2001) 269–289.
- [22] J. Ren, Z. Li, F. Wong, A new method for the prediction of pore size distribution and MWCO of ultrafiltration membranes, *J. Membr. Sci.*, 279 (2006) 558–569.
- [23] Y. Fang, L. Bian, Q. Bi, Q. Li, X. Wang, Evaluation of the pore size distribution of a forward osmosis membrane in three different ways, *J. Membr. Sci.*, 454 (2014) 390–397.
- [24] A.A. Merdaw, A.O. Sharif, G.A.W. Derwish, Mass transfer in pressure-driven membrane separation processes, Part II, *Chem. Eng. J.*, 168 (2011) 229–240.